CHAPTER 6

LEGENDRE WAVELET METHOD ON SIZE DEPENDENT BENDING ANALYSIS OF NANOBEAM UNDER NONLOCAL STRAIN GRADIENT THEORY

6.1 Introduction[1]

The discrepancy between experimental and classical continuum mechanics results arising from a wide variety of nanoscale investigations demonstrates that the classical theory might not be able to accurately predict the response of nanostructures since it does not take into account size-scale parameters. It is therefore meaningful to consider non-classical continuum theories that incorporate extra material length scale parameters in order to characterize the size effect in nanostructures. Additionally, several experimental outcomes and theoretical findings showed that the stiffness enhancement effect is a significant factor in explaining the size-dependent analysis comprehensively.

This chapter of thesis examines the prediction of bending characteristics of the Euler-Bernoulli nanobeam using Moore-Gibson-Thompson thermoelasticity theory in conjunction with nonlocal strain gradient theory (NSGT). This work is motivated from some investigations on size-dependent vibration analysis of small scale structures in the frame of nonlocal theory, nonlocal strain-gradient theory as reported by Zenkour et al.

---

[1]The content of this chapter is communicated to an International Journal.

(2014), Li and Hu (2015), Rezazadeh et al. (2015), Ebrahimi and Barati (2017a), Li et al. (2017), She et al. (2018), Jena et al. (2021), Jena et al. (2022), Mehrparvar et al. (2022), Yang et al. (2023) and Kumar and Mukhopadhyay (2023).

In this chapter, the Legendre wavelet method is employed to analyze the size-dependent thermoelastic bending characteristics of a nanobeam structure by considering coupled thermoelastic equations within the framework of nonlocal strain gradient theory (NSGT) and MGT heat conduction model. The coupled equations for dimensionless deflection and temperature change with ramp-type boundary conditions are formulated and solved using Laplace method and Wavelet approximation method. The stiffness softening and hardening effects due to the nonlocal paramter and length-scale parameter are assessed, and their discrepancies are discussed. The bending nature under different beam theories is finally discussed for various geometrical parameters (nonlocal parameter and length scale parameters) and the comparative analysis on effects of non-local theory and strain gradient theory on deflection and thermal moment of nanobeam structure is presented.

6.2 Theoretical Preliminaries

The rectangular cross-section is assumed with the dimensions of length L, width b, and thickness h corresponding to x, y, and z-axes, respectively, for small deflection.
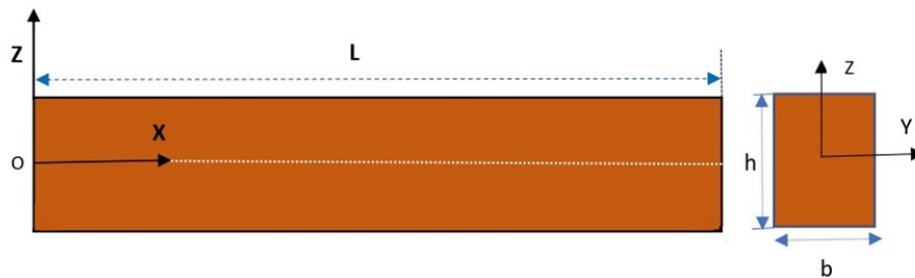

Figure 6.2.1: Graphical illustration of Beam Modeling

6.2.1 The basics of nonlocal strain gradient theory (NSGT)

In Eringen's theory (Eringen (1972; 1983)), the nonlocal effect in classical stress field σ_{ij} depends on strain not only at the reference point but also depend at all domain points. An extended version of this theory is established by Lim et al. (2015) by introducing strain gradient parameter l_s in the constitutive equation of the internal energy density function. According to this proposed theory, total stress tensor $\sigma_{ij}^T(x)$ is the fusion of both non local elastic stress tensor $\sigma_{ij}^{(0)}(x)$ and higher order strain gradient stress tensor $\sigma_{ij}^{(1)}(x)$, which is defined as follows:

$$\sigma_{ij}^T(x) = \sigma_{ij}^{(0)}(x) - \nabla \sigma_{ij}^{(1)}(x), \tag{6.2.1}$$

where $\sigma_{ij}^{(0)}(x)$ and $\sigma_{ij}^{(1)}(x)$ are given by

$$\sigma_{ij}^{(0)}(x) = \int_V \Omega_0\left(x,\,x',\,e_0 a\right) C_{ijkl} e_{kl}(x') dV, \tag{6.2.2}$$

$$\sigma_{ij}^{(1)}(x) = l_s^2 \int_V \Omega_1\left(x,\,x', e_1 a\right) C_{ijkl} e_{kl,m}(x') dV, \tag{6.2.3}$$

$\Omega_0\left(x, x', e_0 a\right)$ and $\Omega_0\left(x, x', e_1 a\right)$ in above equations are two nonlocal functions with nonlocal parameters $e_0 a$ and $e_1 a$. C_{ijkl} stands for the elastic modulus tensor of fourth order. $e_{kl}(x')$ and $e_{kl,m}(x')$ are strain tensor and higher order strain gradient tensor at reference point x', respectively. l_s denotes the strain gradient parameter to show the relevance of the higher order strain gradient stress field. According to linear thermoelasticity, the linear thermoelastic constitutive relation of local stress field component $\sigma_{ij}(x')$ is given as

$$\sigma_{ij}(x') = 2\mu e_{ij}(x') + \{\lambda e_{kk}(x') - (3\lambda + 2\mu)\,\alpha_t \theta\}\,\delta_{ij}, \tag{6.2.4}$$

where e_{kk} is volumetric part of strain tensor, α_t is linear thermal expansion coefficient, and $\theta = T - T_0$ is the temperature excess of system at time t. $\lambda = \frac{E\vartheta}{(1+\vartheta)(1-2\vartheta)}$ and $\mu = \frac{E}{2(1+\vartheta)}$ are the Lame's constants.

Here, ϑ is Poisson's ratio and E refers to the elastic modulus. The following forms define the linear nonlocal differential operator, which could be utilized with nonlocal functions (Lim et al. (2015)):

$$L_1 = \left(1 - \left(\frac{e_0 a}{L}\right)^2 L^2 \frac{\partial^2}{\partial x^2}\right), \tag{6.2.5}$$

$$L_2 = \left(1 - \left(\frac{e_1 a}{L}\right)^2 L^2 \frac{\partial^2}{\partial x^2}\right), \tag{6.2.6}$$

where L represents the length of the beam.

Further, in view of Eqs. (6.2.5) and (6.2.6), a simplified form of Eqs. (6.2.2) and (6.2.3) can be found as follows (Lim et al. (2015)):

$$L_1 \sigma_{ij}^{(0)}(x) = \sigma_{ij}(x'), \tag{6.2.7}$$

$$L_2 \sigma_{ij}^{(1)}(x) = l_s^2 \nabla \sigma_{ij}(x'). \tag{6.2.8}$$

By combining Eqs. (6.2.4), (6.2.7) and (6.2.8) for $e_0 = e_1$, it is obtained that

$$\left(1 - \eta L^2 \nabla^2\right) \sigma_{ij}^{(0)}(x) = 2\mu e_{ij}(x') + \{\lambda e_{kk}(x') - \beta\theta\} \delta_{ij}, \tag{6.2.9}$$

$$\left(1 - \eta L^2 \nabla^2\right) \sigma_{ij}^{(1)}(x) = \tau^2 L^2 \{2\mu \nabla e_{ij}(x') + (\lambda \nabla e_{kk}(x') - \beta\nabla\theta) \delta_{ij}\}, \tag{6.2.10}$$

where $\eta = \frac{e_0 a}{L}$ and $\tau = \frac{l_s}{L}$ are dimensionless nonlocal and strain gradient parameters, respectively. Moreover, $\beta = \frac{E\alpha_t}{(1-2\vartheta)}$ is the thermoelastic coupling parameter.

In view of Eqs. (6.2.9) and (6.2.10), the following is acquired:

$$\left(1 - \eta L^2 \nabla^2\right) \sigma_{ij}^{(T)}(x) = 2\mu e_{ij}(x') + \{\lambda e_{kk}(x') - \beta\theta\} \delta_{ij} - \tau^2 L^2 \nabla^2 \{2\mu e_{ij}(x') + (\lambda e_{kk}(x') - \beta\theta) \delta_{ij}\}.$$
(6.2.11)

In the special case when the thermal effect is negligible (i.e., $\alpha_t = 0$) in above equation, then one can obtain the constitutive relation for NSGT as

$$\left(1 - \eta^2 L^2 \frac{\partial^2}{\partial x^2}\right) \sigma_{xx}^T(x) = (\lambda + 2\mu) \left(1 - \tau^2 L^2 \frac{\partial^2}{\partial x^2}\right) e_{xx}(x').$$
(6.2.12)

The above constitutive relation can be characterized by three different theories:

- Classical Elasticity theory (CT): $\sigma_{ij}^T(x) = (\lambda + 2\mu) e_{kk}(x')$ when $\eta = 0$ and $\tau = 0$.

- Nonlocal beam theory (NBT): $\{1 - \eta^2 L^2 \nabla^2\} \sigma_{ij}^T(x) = (\lambda + 2\mu) e_{kk}(x')$ when $\eta \neq 0$ and $\tau = 0$.

- Strain gradient theory (SGT): $\sigma_{ij}^T(x) = (\lambda + 2\mu) (1 - \tau^2 L^2 \nabla^2) e_{kk}(x')$ when $\eta = 0$ and $\tau \neq 0$.

6.2.2 Equation of motion of nanobeam resonator

The Euler-Bernoulli nanobeam is considered in this chapter. Therefore, the displacement components are assumed to have the form as

$$u_x = -z \frac{\partial w(x,t)}{\partial x}, \quad u_y = 0, \quad u_z = w(x,t),$$
(6.2.13)

where $w(x,t)$ is small transverse deflection. By using plane stress condition, the normal strain components are given as

$$e_{xx} = -z \frac{\partial^2 w(x,t)}{\partial x^2}, \quad e_{yy} = 0, \quad e_{zz} = 0.$$

Therefore, non-vanishing volumetric strain can be obtained as

$$e_{kk} = -z\frac{\partial^2 w(x,t)}{\partial x^2}. \tag{6.2.14}$$

Putting Eq. (6.2.14) into Eq. (6.2.11), the constitutive relation for NSGT with thermal effect takes form as

$$\left(1 - \eta^2 L^2 \frac{\partial^2}{\partial x^2}\right)\sigma_{xx}^T(x) = \left\{(\lambda + 2\mu)\left(1 - \tau^2 L^2 \frac{\partial^2}{\partial x^2}\right)\left(-z\frac{\partial^2 w(x,t)}{\partial x^2}\right) - \beta\theta\right\}. \tag{6.2.15}$$

Now, multiplying Eq. (6.2.15) by z and integrating the result with respect to cross-sectional area dA, the following is achieved:

$$\left\{1 - \eta^2 L^2 \frac{\partial^2}{\partial x^2}\right\}M = -\left\{(\lambda + 2\mu)I\left(1 - \tau^2 L^2 \frac{\partial^2}{\partial x^2}\right)\frac{\partial^2 w(x,t)}{\partial x^2} + M_t\right\}, \tag{6.2.16}$$

where $I = \frac{bh^3}{12}$ is moment of inertia. The bending moment M and thermal moment M_t are given by

$$M_t = E\alpha_t b \int_{-h/2}^{h/2} \theta z \, dz, \tag{6.2.17}$$

$$M = \iint \sigma_{xx}^T(x) z \, dA. \tag{6.2.18}$$

An Euler-Bernoulli beam vibrating transversely can be described by the following equation of motion (see Lim et al. (2015), Rezazadeh et al. (2015)):

$$\frac{\partial^2 M}{\partial x^2} - \rho A \frac{\partial^2 w(x,t)}{\partial t^2} = 0, \tag{6.2.19}$$

where ρ is the mass density.

In view of Eqs. (6.2.16) and (6.2.19), the equation of motion is derived by using NSGT

theory as follows:

$$S_1 \frac{\partial^4 w}{\partial x^4} + S_2 \frac{\partial^2 w}{\partial t^2} + \frac{\partial^2 M_t}{\partial x^2} = 0, \tag{6.2.20}$$

where $S_1 = (\lambda + 2\mu) I \left(1 - \tau^2 L^2 \frac{\partial^2}{\partial x^2}\right)$ and $S_2 = \rho A \left(1 - \eta^2 L^2 \frac{\partial^2}{\partial x^2}\right)$.

6.2.3 Coupled heat conduction equation for the Moore–Gibson–Thompson (MGT) Theory

Using non-vanishing strain components e_{kk} in the MGT heat conduction equation, it is obtained that

$$\left(K \frac{\partial}{\partial t} + K^*\right) \left(\frac{\partial^2 \theta}{\partial x^2} + \frac{\partial^2 \theta}{\partial z^2}\right) - \left(1 + \tau_q \frac{\partial}{\partial t}\right) \left(\rho c_E \frac{\partial^2}{\partial t^2} \theta - T_0 \beta z \frac{\partial^4 w}{\partial t^2 \partial x^2}\right) = 0. \tag{6.2.21}$$

The above equation takes the following form by multiplying with $b\beta z$ and then integrating the resultant over the thickness direction:

$$\left(K \frac{\partial}{\partial t} + K^*\right) \left(\frac{\partial^2 M_t}{\partial x^2} + b\beta \int\limits_{-h/2}^{h/2} z \frac{\partial^2 \theta}{\partial z^2} dz\right) - \left(1 + \tau_q \frac{\partial}{\partial t}\right) \left(\rho c_E \frac{\partial^2}{\partial t^2} M_t - I T_0 \beta^2 \frac{\partial^4 w}{\partial t^2 \partial x^2}\right) = 0. \tag{6.2.22}$$

6.3 Deflection and Temperature Field

The temperature change in thin beam vary along the z- axes (thickness direction) as the function of $\sin(gz)$. Therefore, we can express θ in the following form:

$$\theta(x, z, t) = \Theta(x, t) \sin(gz), \tag{6.3.1}$$

where $g = \frac{\pi}{h}$.

Then, Eqs. (6.2.20) and (6.2.22) take the following forms:

$$\rho A \frac{\partial^2 w}{\partial t^2} - \eta^2 L^2 \rho A \frac{\partial^4 w}{\partial t^2 \partial x^2} + (\lambda + 2\mu) I \frac{\partial^4 w}{\partial x^4} - (\lambda + 2\mu) I \tau^2 L^2 \frac{\partial^6 w}{\partial x^6} + \frac{2b\beta}{g^2} \frac{\partial^2 \Theta}{\partial x^2} = 0,$$

(6.3.2)

$$\left(K \frac{\partial}{\partial t} + K^* \right) \left(\frac{\partial^2 \Theta}{\partial x^2} - g^2 \Theta \right) - \left(1 + \tau_q \frac{\partial}{\partial t} \right) \left(\rho c_E \frac{\partial^2 \Theta}{\partial t^2} - \frac{I T_0 \beta g^2}{2b} \frac{\partial^4 w}{\partial t^2 \partial x^2} \right) = 0.$$

(6.3.3)

Here, the following dimensionless variables are used for convenience:

$$x' = \frac{x}{L}, \quad t' = \frac{t\epsilon}{L} \quad w' = \frac{w}{h}, \quad \theta' = \frac{\Theta}{T_0},$$

$$\eta = \frac{e_0 a}{L}, \quad \tau = \frac{l_s}{L}, \quad \epsilon = \sqrt{\frac{E}{\rho}}, \quad \tau_1' = \frac{\tau_q \epsilon}{L}.$$

By taking these non-dimensional variables and notations and omitting the primes for simplicity, Eqs. (6.3.2) and (6.3.3) yield the following equations:

$$\frac{\partial^2 w}{\partial t^2} - \mathcal{L}_1 \frac{\partial^4 w}{\partial t^2 \partial x^2} + \mathcal{L}_2 \frac{\partial^4 w}{\partial x^4} - \mathcal{L}_3 \frac{\partial^6 w}{\partial x^6} + \mathcal{L}_4 \frac{\partial^2 \theta}{\partial x^2} = 0,$$

(6.3.4)

$$\left(k_1 + \frac{\partial}{\partial t} \right) \left(\frac{\partial^2 \theta}{\partial x^2} - \mathcal{L}_5 \theta \right) - \left(1 + \tau_1 \frac{\partial}{\partial t} \right) \left(\mathcal{L}_6 \frac{\partial^2 \theta}{\partial t^2} - \mathcal{L}_7 \frac{\partial^4 w}{\partial t^2 \partial x^2} \right) = 0,$$

(6.3.5)

where

$$k_1 = \frac{K^* L}{K \epsilon}, \quad \mathcal{L}_1 = \eta^2, \quad \mathcal{L}_2 = \frac{(\lambda + 2\mu) I}{L^2 EA}, \quad \mathcal{L}_3 = \frac{(\lambda + 2\mu) I \tau^2}{L^2 EA}, \quad \mathcal{L} = 2 \frac{T_0 b \beta}{g^2 EAh},$$

$$\mathcal{L}_5 = g^2 L^2, \quad \mathcal{L}_6 = \frac{\rho c_E E L \epsilon}{K}, \quad \mathcal{L}_7 = \frac{\beta I g^2 h \epsilon}{2b K L}.$$

Further, the initial conditions are taken to be homogeneous and boundary conditions in dimensionless forms are considered as follows:

$$w(0,t) = \frac{\partial^2 w}{\partial x^2}(0,t) = \frac{\partial^4 w}{\partial x^4}(0,t) = 0; \quad w(1,t) = \frac{\partial^2 w}{\partial x^2}(1,t) = \frac{\partial^4 w}{\partial x^4}(1,t) = 0, \quad (6.3.6)$$

$$\theta(0,t) = \theta_0 \begin{cases} 0 & \text{for} \quad t \le 0 \\ \frac{t}{t_0} & \text{for} \quad 0 < t < t_0 \\ 1 & \text{for} \quad t \ge t_0 \end{cases}, \quad \theta(1,\bar{t}) = 0. \quad (6.3.7)$$

where t_0 is non negative ramp time parameter and θ_0 is a fixed constant temperature.

6.4 Legendre Wavelets

The mother wavelet $\Psi(x)$ plays a vital role in generating a set of functions, called wavelets, by translation and dilation. The dilation parameter c and translation parameter d are continually varied to produce the family of continuous wavelets in the following way (Daubechies (1992)):

$$\Psi_{c,d}(x) = |c|^{-1/2} \Psi\left(\frac{x-d}{c}\right),$$

where $c,d \in \mathbb{R}$ and $c \ne 0$.

Legendre wavelets $\Psi_{m,n}(x) = \Psi(n,r,\hat{m},x)$ in the context of Legendre polynomials $L_n(x)$ of order n, which belong to the interval $[-1,1]$ is defined as follows (Liu and Lin (2010), Xu and Xu (2018)):

$$\Psi_{m,n}(x) = \begin{cases} \sqrt{n+\frac{1}{2}}\, 2^{\frac{r}{2}} L_n(2^r x - \hat{m}), & \frac{\hat{m}-1}{2^r} \le x < \frac{\hat{m}}{2^r} \\ 0, & \text{otherwise} \end{cases}, \quad (6.4.1)$$

where $x \in [0,1)$ and the coefficient $\sqrt{n+\frac{1}{2}}$ is taken for orthonormality. Moreover,

$r \in \mathbb{N}$, $m = 1, 2, ..., 2^{r-1}$, $\hat{m} = 2m - 1$, $n = 0, 1, 2, ..., N - 1$ is the order of Legendre polynomial.

6.4.1   Function approximation

In the form of Legendre wavelet, any function $u(x) \in L^2(\mathbb{R})$ defined on the interval $[0, 1)$ can be represented as

$$u(x) = \sum_{m=1}^{\infty} \sum_{n=0}^{\infty} \beta_{m,n} \Psi_{m,n}(x), \tag{6.4.2}$$

where $\beta_{m,n} = \langle u(x), \Psi_{m,n}(x) \rangle$ denote the wavelet coefficients and $\langle ., . \rangle$ is the inner product in $L^2[0, 1)$.

If the above series defined in Eq. (6.4.2) is truncated, it is simplified to the following form:

$$u(x) \cong \sum_{m=1}^{2^{r-1}} \sum_{n=0}^{N-1} \beta_{m,n} \Psi_{m,n}(x).$$

By using concise notation, it can be defined as follows:

$$u(x) \cong \sum_{i=1}^{\hat{n}} \beta_i \Psi_i(x) = B^T \Psi(x),$$

where B and $\Psi(x)$ are $\hat{n} = 2^{r-1} N$ column vectors defined as

$$B = [\beta_{1,0}, \beta_{1,1}, ..., \beta_{1,N-1}, \beta_{2,0}, ..., \beta_{2,N-1}, ..., \beta_{2^{r-1},0}, \beta_{2^{r-1},1}, ..., \beta_{2^{r-1},N-1}]^T,$$

$$\Psi(x) = [\Psi_{1,0}, \Psi_{1,1}, ..., \Psi_{1,N-1}, \Psi_{2,0}, ..., \Psi_{2,N-1}, ..., \Psi_{2^{r-1},0}, \Psi_{2^{r-1},1}, ..., \Psi_{2^{r-1},N-1}]^T.$$

6.4.2   Convergence of Legendre wavelets

Theorem (Liu and Lin (2010)): A continuous function $u(x)$ defined on $[0, 1]$ can be written as an infinite sum of Legendre wavelets, and the series converges uniformly to

$u(x)$ if it has a bounded second-order derivative., i.e.

$$u(x) = \sum_{m=1}^{\infty} \sum_{n=0}^{\infty} \beta_{m,n} \Psi_{m,n}(x).$$

Proof: (see Liu and Lin (2010)).

6.5 Solution Procedure

Here, the Laplace transform method and Wavelet method are used to solve the Eqs. (6.3.4) and (6.3.5). Applying the Laplace transform

$$\mathcal{L}[u(x,t)] = \overline{u}(x,p) = \int_0^{\infty} u(x,t)e^{-pt}dt$$

to the Eqs. (6.3.4) and (6.3.5) by utilizing the homogeneous initial conditions, it is obtained that

$$p^2\overline{w} - \mathcal{L}_1 p^2 \frac{\partial^2 \overline{w}}{\partial x^2} + \mathcal{L}_2 \frac{\partial^4 \overline{w}}{\partial x^4} - \mathcal{L}_3 \frac{\partial^6 \overline{w}}{\partial x^6} + \mathcal{L}_4 \frac{\partial^2 \overline{\theta}}{\partial x^2} = 0, \qquad (6.5.1)$$

$$(k_1 + p)\left(\frac{\partial^2 \overline{\theta}}{\partial x^2} - \mathcal{L}_5 \overline{\theta}\right) - (1 + \tau_1 p)\left(\mathcal{L}_6 p^2 \overline{\theta} - \mathcal{L}_7 p^2 \frac{\partial^2 \overline{w}}{\partial x^2}\right) = 0, \qquad (6.5.2)$$

where p is the Laplace transform parameter.

Similarly, Laplace transform is applied to boundary conditions (6.3.6) and (6.3.7) to get the following equations

$$\overline{w}(0,p) = \frac{\partial^2 \overline{w}}{\partial x^2}(0,p) = \frac{\partial^4 \overline{w}}{\partial x^4}(0,p) = 0, \qquad (6.5.3)$$

$$\overline{w}(1,p) = \frac{\partial^2 \overline{w}}{\partial x^2}(1,p) = \frac{\partial^4 \overline{w}}{\partial x^4}(1,p) = 0, \qquad (6.5.4)$$

$$\overline{\theta}(0,p) = \frac{\theta_0}{t_0 p^2} - \frac{\theta_0 e^{-pt_0}}{t_0 p^2}, \quad \overline{\theta}(1,p) = 0, \qquad (6.5.5)$$

6.5.1 Space discretization by Legendre wavelets

The Legendre wavelet method is adopted to approximate the space domain in this subsection. In wavelet-based approaches, wavelet series is often used to approximate the highest order derivative of an unknown function that appears in the problem. After that, using boundary conditions and sequential integration, the unknown function itself as well as its lower-order derivatives are obtained. Following this, it is assumed that $\frac{\partial^6 \overline{w}}{\partial x^6}$ can be expressed by Legendre wavelet in the following way (Liu and Lin (2010), Xu and Xu (2018)):

$$\frac{\partial^6 \overline{w}}{\partial x^6}(x, p) = \sum_{i=1}^{\hat{n}} a_i \Psi_i(x). \tag{6.5.6}$$

In order to solve this further, the following notations are used (Oruç et al. (2015)):

$$P_{i,1}(x) = \int_0^x \Psi_i(\xi)d\xi, \;\; P_{i,2}(x) = \int_0^x P_{i,1}(\xi)d\xi, \;\; P_{i,3}(x) = \int_0^x P_{i,2}(\xi)d\xi,$$

$$P_{i,4}(x) = \int_0^x P_{i,3}(\xi)d\xi, \;\; P_{i,5}(x) = \int_0^x P_{i,4}(\xi)d\xi, \;\; P_{i,6}(x) = \int_0^x P_{i,5}(\xi)d\xi. \tag{6.5.7}$$

Now, integrating Eq. (6.5.6) with respect to x from 0 to x and using Eq. (6.5.7), we obtain

$$\frac{\partial^5 \overline{w}}{\partial x^5}(x, p) = \sum_{i=1}^{\hat{n}} a_i P_{i,1}(x) + \frac{\partial^5 \overline{w}}{\partial x^5}(0, p). \tag{6.5.8}$$

Again integrating above equation two times with respect to x from 0 to x and using Eq. (6.5.7) and boundary condition given by Eq. (6.5.3), it is acquired that

$$\frac{\partial^4 \overline{w}}{\partial x^4}(x, p) = \sum_{i=1}^{\hat{n}} a_i P_{i,2}(x) + x \frac{\partial^5 \overline{w}}{\partial x^5}(0, p), \tag{6.5.9}$$

since $\frac{\partial^5 \overline{w}}{\partial x^5}(0, p)$ is unknown in above equation so by substituting $x = 1$ in above equation and using boundary condition, Eq. (6.5.9) yields

$$\frac{\partial^4 \overline{w}}{\partial x^4}(x, p) = \sum_{i=1}^{\hat{n}} a_i P_{i,2}(x) - x \sum_{i=1}^{\hat{n}} a_i P_{i,2}(1). \tag{6.5.10}$$

Now, taking double integration of Eq. (6.5.10) with respect to x, the following is achieved:

$$\frac{\partial^2 \overline{w}}{\partial x^2}(x,p) = \sum_{i=1}^{\hat{n}} a_i P_{i,4}(x) - \frac{x^3}{6} \sum_{i=1}^{\hat{n}} a_i P_{i,2}(1) - x \sum_{i=1}^{\hat{n}} a_i P_{i,4}(1) + \frac{x}{6} \sum_{i=1}^{\hat{n}} a_i P_{i,2}(1). \quad (6.5.11)$$

Again integrating two times Eq. (6.5.11) with respect to x and considering Eqs. (6.5.4), (6.5.5) and (6.5.7), the following is obtained:

$$\overline{w}(x,p) = \sum_{i=1}^{\hat{n}} a_i P_{i,6}(x) - \frac{x^5}{120} \sum_{i=1}^{\hat{n}} a_i P_{i,2}(1) - \frac{x^3}{6} \sum_{i=1}^{\hat{n}} a_i P_{i,4}(1) + \frac{x^3}{36} \sum_{i=1}^{\hat{n}} a_i P_{i,2}(1)$$
$$- x \left(\sum_{i=1}^{\hat{n}} a_i P_{i,6}(1) - \frac{1}{120} \sum_{i=1}^{\hat{n}} a_i P_{i,2}(1) - \frac{1}{6} \sum_{i=1}^{\hat{n}} a_i P_{i,4}(1) + \frac{1}{36} \sum_{i=1}^{\hat{n}} a_i P_{i,2}(1) \right).$$
$$(6.5.12)$$

Similarly, $\frac{\partial^2 \overline{\theta}}{\partial x^2}$ is expanded by Legendre wavelets as follows:

$$\frac{\partial^2 \overline{\theta}}{\partial x^2}(x,p) = \sum_{i=1}^{\hat{n}} b_i \Psi_i(x). \quad (6.5.13)$$

Also, by double integrating Eq. (6.5.13) with respect to x from 0 to x, the following equation is acquired:

$$\overline{\theta}(x,p) = \sum_{i=1}^{\hat{n}} b_i P_{i,2}(x) + x \frac{d\overline{\theta}}{dx}(0,p) + \overline{\theta}(0,p). \quad (6.5.14)$$

Now by putting $x = 1$ in the above equations and making use of boundary conditions given by Eq. (6.5.5), it is obtained that

$$\overline{\theta}(x,p) = \sum_{i=1}^{\hat{n}} b_i P_{i,2}(x) - x \sum_{i=1}^{\hat{n}} b_i P_{i,2}(1) - (x-1) \left(\frac{\theta_0}{t_0 p^2} - \frac{\theta_0 e^{-pt_0}}{t_0 p^2} \right). \quad (6.5.15)$$

Substituting Eqs. (6.5.6), (6.5.10)-(6.5.13) and (6.5.15) into Eqs. (6.5.1) and (6.5.2) and discretizing the space variable x in collocation points $\frac{2i-1}{2\hat{n}}$, $i = 1, 2, ..., \hat{n}$, a system

of algebraic equations is found which can be represented in the following matrix form:

$$\mathscr{P}\boldsymbol{X} = \boldsymbol{Q}, \tag{6.5.16}$$

where $\mathscr{P}$ is a $2\hat{n} \times 2\hat{n}$ matrix of known coefficients, Q is known matrix of order $2\hat{n} \times 1$ and $\boldsymbol{X}$ denotes the following vector of wavelet coefficients:

$$\boldsymbol{X} = [a_{1,0}, a_{1,1}, ..., a_{2^{r-1},0}, ..., a_{2^{r-1},N-1}, b_{1,0}, b_{1,1}, ..., b_{2^{r-1},0}, ..., b_{2^{r-1},N-1}]^T .$$

From Eq. (6.5.16), wavelet coefficients $\boldsymbol{X}$ are obtained. Then, by plugging these wavelet coefficients into Eqs. (6.5.12) and (6.5.15), the solutions for deflection and temperature are constructed in Laplace transform domain.

6.5.2   Inversion of Laplace transform

In order to obtain the numerical solutions for deflection and change in temperature for the time domain, the numerical inversion of the Laplace transform is adopted. For this purpose, the approach of numerical inversion is used based on the Stehfest method (Stehfest (1970)). In this approach, the inverse of a function $\overline{u}(x, p)$ can be evaluated in time domain as

$$u(x, t) = \frac{\ln 2}{t} \sum_{j=1}^{2M} N_j \overline{u}\left(x, \frac{j \ln 2}{t}\right), \tag{6.5.17}$$

with

$$N_j = (-1)^{m+M} \sum_{k=\left[\frac{m+1}{2}\right]}^{\min\left(m, \frac{M}{2}\right)} \frac{k^{\frac{M}{2}}(2k)!}{(\frac{M}{2} - k)!k!(m-k)!(2k-1)!}, \tag{6.5.18}$$

where M is an integer and $\left[\frac{m+1}{2}\right]$ denotes the integer part of real number $\frac{m+1}{2}$.

6.6 Numerical results and discussion

In this section, the bending analysis of the silicon nano-resonator is investigated by the Legendre wavelet method under nonlocal strain gradient theory. The dimensionless terms of deflection and temperature changes in beam resonator are studied under the recent MGT thermoelasticity theory. Now, in order to illustrate the problem and examine the effects of nonlocal parameter, length scale parameter, aspect ratio, and ramp type parameter on the responses of deflection and temperature, computational work is carried out on the basis of the analytical solution as obtained in the previous section. The following numerical data at reference temperature $T_0 = 293K$ is used here for finding the nature of several comparisons:

$$E = 169\,\text{GPa},\ c_E = 713\,\text{J/kgK},\ \rho = 2330\,\text{kg/m}^3,\ \alpha_t = 2.59{\times}10^{-6}\text{K}^{-1},\ K = K^* = 156\,\text{W/mK}.$$

Numerical computations and graphical outputs are achieved using MATLAB software. The numerical solutions of the present problem are demonstrated in various graphs for the values of $r = 1$ and $N = 6$.

6.6.1 Validation of numerical results

For the cases of deflection and temperature distribution, the results of the current findings are compared with the results of Zenkour et al. (2014) in Figs. 6.6.1(a,b). Zenkour et al. (2014) obtained the vibration behavior of nanobeam in the context of a refined nonlocal thermoelasticity theory for the LS heat conduction model. This is a particular case of the present study as by making $K^* = 0$ in the MGT heat conduction equation, results for the LS thermoelasticity theory is derived. From Figs. 6.6.1(a,b), it is revealed that how effectively the current study agrees with the results reported by Zenkour et al. (2014). It can be observed that the temperature distribution and

deflection agree well. This shows that the current numerical procedure is accurate and effective.
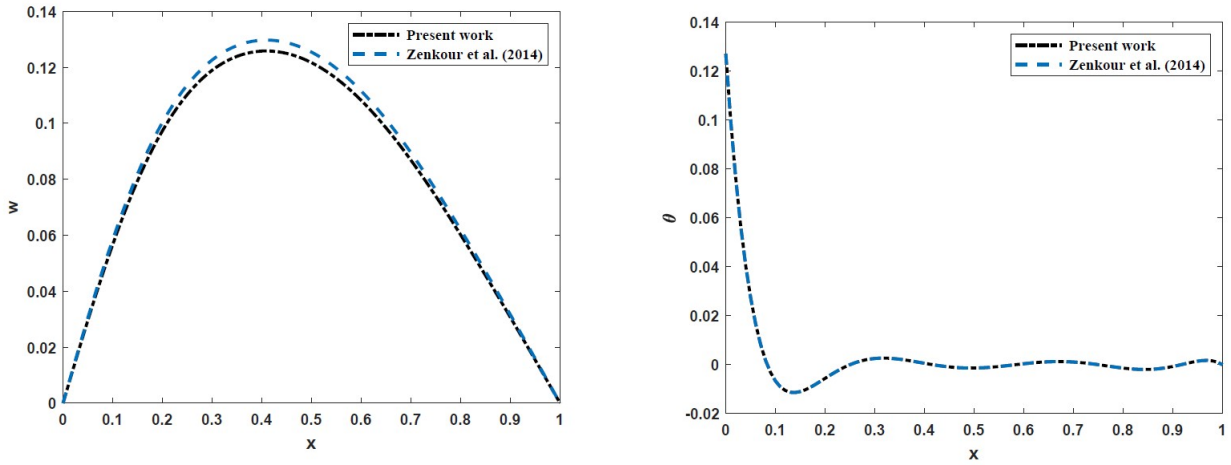

Figure 6.6.1: Comparison of deflection and temperature change between present work and the work by Zenkour et al. (2014)

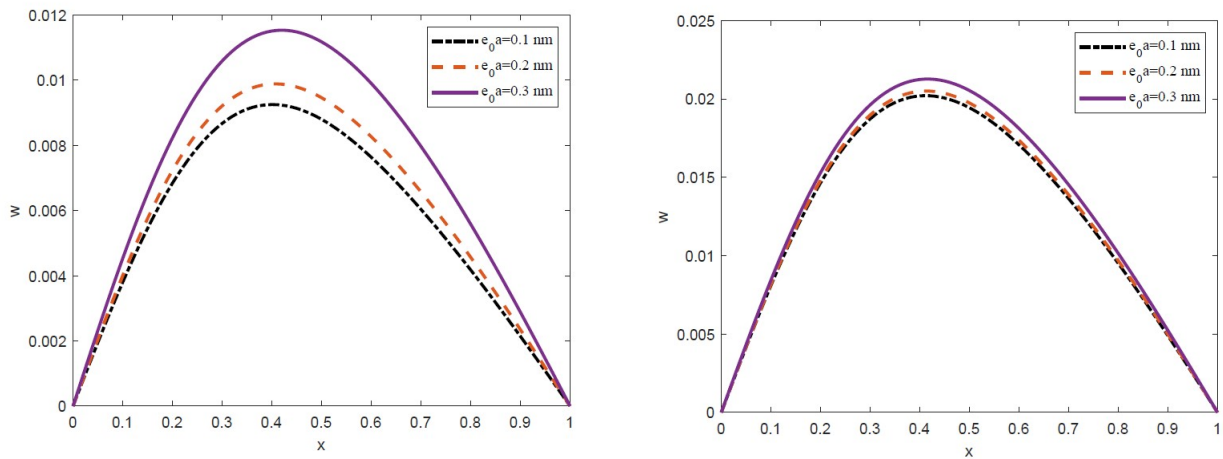## 6.6.2 Nonlocal effect in deflection

Figure 6.6.2: (a) Effect of nonlocal parameter in normalized deflection at time $t = 25$. (b) Effect of nonlocal parameter in normalized deflection at time $t = 50$.

Figs. 6.6.2(a,b) are plotted to show the dimensionless deflection along with distance x at two different dimensionless times $t = 25$ and 50. Here, the non-negative constants $t_0 = 50$, $b = 0.5 \times h$, $\frac{L}{h} = 10$ and $\theta_0 = 0.1$ are considered. It is observed that with intensifying the nonlocal parameter $e_0 a$, the non-dimensional deflection w is significantly influenced. It is further observed that the deflection ascends to larger maximum when small scale parameter $e_0 a$ increases. Moreover, it is shown that the deflection gets higher value as time increases. The stiffness softening effect due to the nonlocal parameter is clearly seen in both the graphs 6.6.2(a,b).

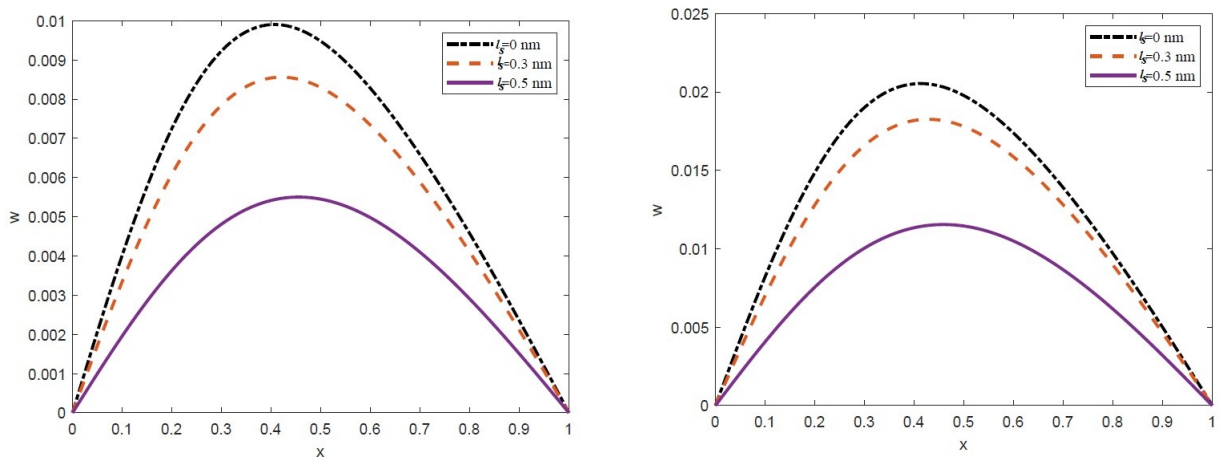### 6.6.3 Effect of length scale parameter

Figure 6.6.3: (a) Effect of strain gradient parameter l_s on dimensionless deflection at time $t = 25$. (b) Effect of strain gradient parameter l_s on dimensionless deflection at time $t = 50$.

Figs. 6.6.3(a,b) are depicted to demonstrate the effects of strain gradient parameter l_s in bending of nanobeam with respect to x at two different time t. This figure displays non-dimensional deflection w for the three level values of length scale parameter l_s (i.e, $l_s = 0, 0.3, 0.5$ nm), where the nonlocal parameter is kept fixed as $e_0 a = 0.2$ nm. It is

well known that the effect of nonlocal and length scale parameters is characterized based on material molecular behavior. It is important to note from the figure that whenever enhancing the length scale parameter, the opposite effect is observed in comparison to the nonlocal effect because enhancing it reduces peaks of deflection. Hence, when the strain gradient parameter is taken into account, the stiffness-hardening nature of beam resonator is illustrated. Also, it is noted that larger amplitude of deflection is attained as time increases.

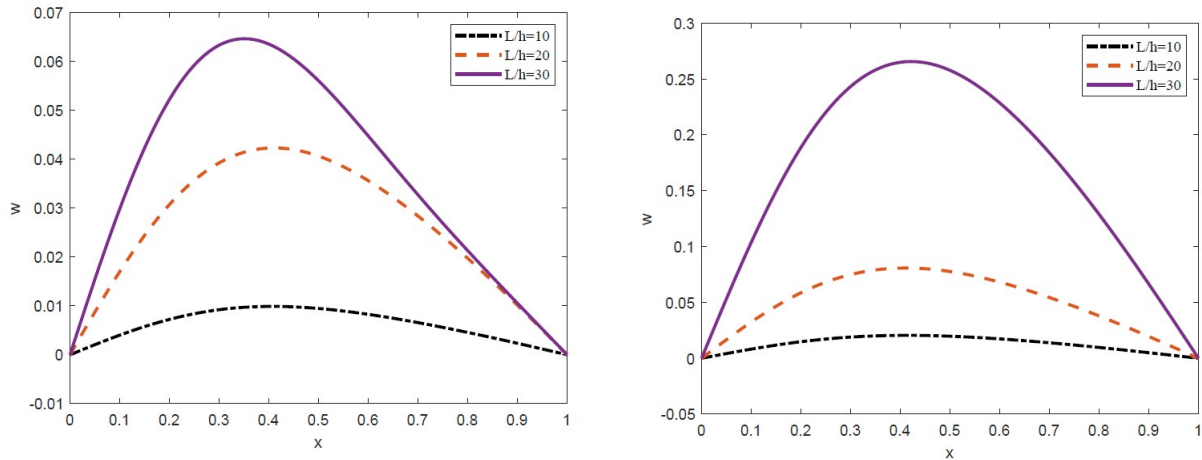### 6.6.4   Effect of different aspect ratio $\frac{L}{h}$

Figure 6.6.4: (a) Effect of different aspect ratio $\frac{L}{h}$ on deflection when $l_s > e_0 a$. (b) Effect of different aspect ratio $\frac{L}{h}$ on deflection when $l_s < e_0 a$.

Figs. 6.6.4(a,b) are focused on illustrating the effect of three-level aspect ratios $\frac{L}{h}$ ($\frac{L}{h} = 10, 20, 30$) on dimensionless deflection w. It is clearly noted that the nonlocal and strain gradient length scale parameters affect amplitudes of deflection differently. When the strain gradient parameter is greater than the nonlocal parameter (i.e., $l_s > e_0 a$), the resonator exhibits a lower value of the amplitude of vibration, which shows the stiffness hardening effect. In the case of $l_s < e_0 a$, the amplitude of dimensionless

deflection ascends, which is responsible for stiffness-softening. Moreover, one can find that the deflection peaks get a higher value when aspect ratio increases. In this case, the oscillation frequency of the beam resonator shrink, which causes more energy dissipation during vibration. The peak values of deflection are attained at a larger distance when $l_s > e_0 a$.

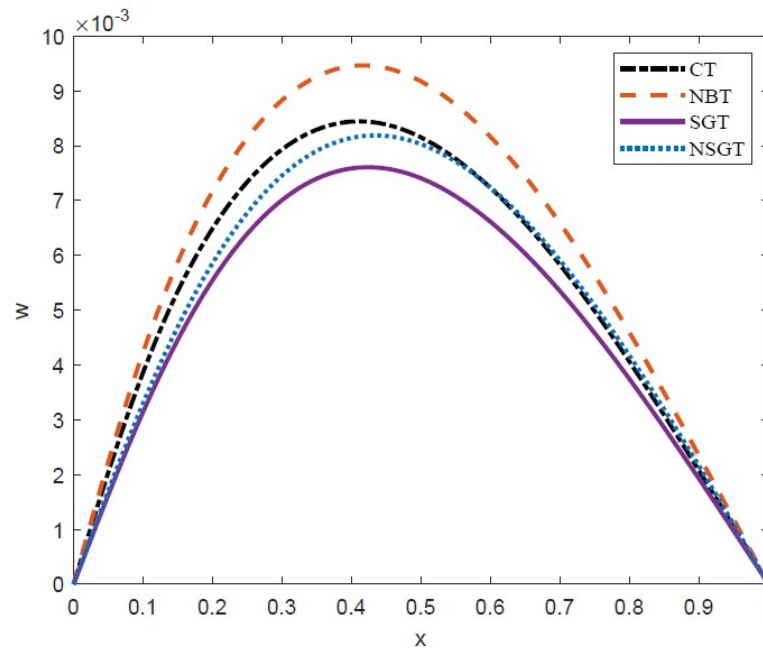### 6.6.5   Deflection and temperature under different theories

Figure 6.6.5: Deflection under different classical and non-classical theories at $t = 25$.

Fig. 6.6.5 depicts the range of dimensionless deflection modeled by classical elasticity theory (CT), nonlocal beam theory (NBT), strain gradient theory (SGT), and the present theory (NSGT) with respect to space variable x. The magnitude of $e_0 a$ and l_s are assumed to be 0.1 nm and 0.5 nm, respectively. It is shown that the maximum span of amplitude is extracted under NBT, while the lowest range of deflection occurs for SGT. In terms of stiffness behavior, SGT and NBT theories have the highest and

lowest values, respectively. The sensitivity of dimensionless temperature θ for various continuum and non-continuum theories is illustrated in Fig. 6.6.6. It is observed that the parameters l_s and $e_0 a$ have no influence on dimensionless temperature. Therefore, the CT, NBT, SGT, and NSGT theories demonstrate exactly the similar behavior of temperature.
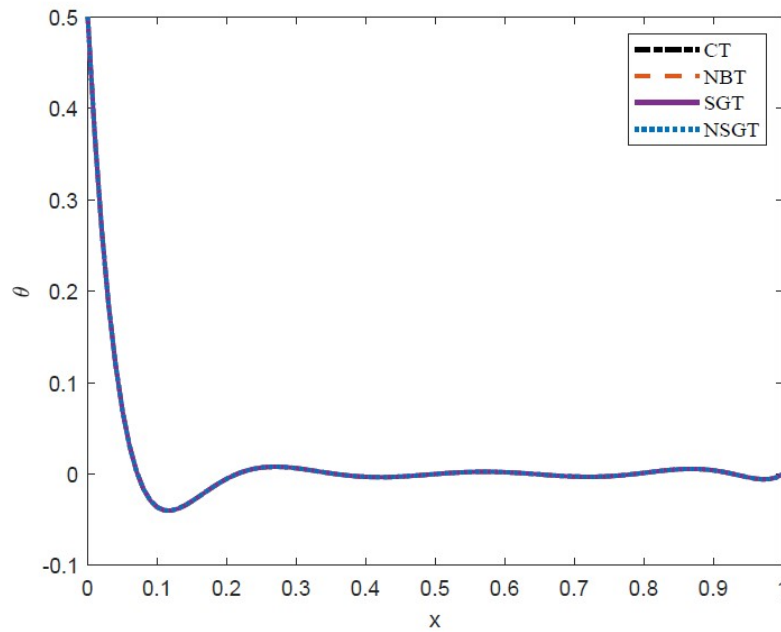

Figure 6.6.6: Temperature under different classical and non-classical theories at $t = 25$.

6.6.6   Effect of ramp time parameter t_0

Fig. 6.6.7 shows the influence of ramp time parameter t_0 ($t_0 = 25, 50, \text{and } 75$) on the deflection w for $t = 25$, whereas the behavior of temperature θ for different ramping parameter is displayed in Fig. 6.6.8. From Fig. 6.6.7, it is concluded that as ramping parameter t_0 increases, deflection decreases. It is further detected that temperature in magnitude decreases with the increase in ramping parameter. This is clearly verified in Fig. 6.6.8. Hence, the non-dimensional deflection and temperature are observed to be significantly impacted by the ramping time parameter t_0.
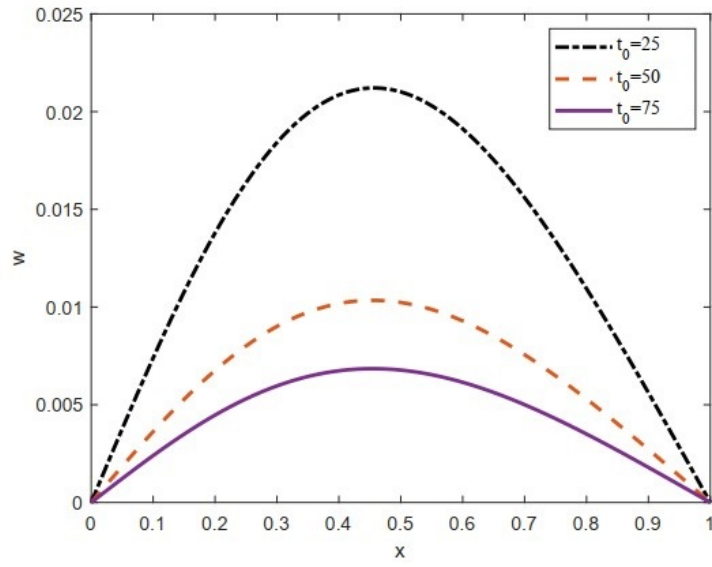
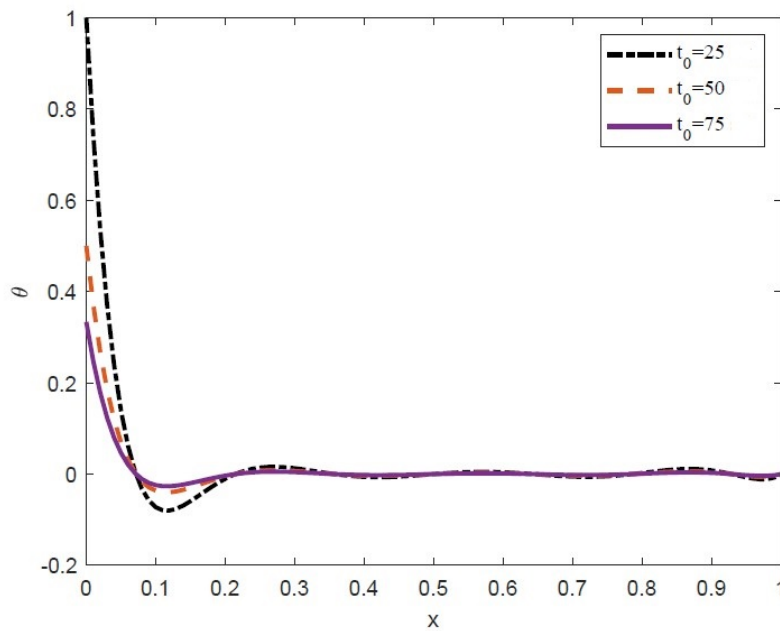Figure 6.6.7: Effect of ramp type parameter t_0 on deflection at time $t = 25$.

Figure 6.6.8: Effect of ramp type parameter t_0 on temperature at time $t = 25$.

6.7   Conclusion

This work analyzes the bending and temperature changes of nanobeam resonators under the higher order nonlocal strain gradient (non-continuum) theory and the MGT thermoelasticity model. The Legendre Wavelet method combined with the Laplace transform technique is utilized to get the numerical solutions of coupled partial differential equations. Validation of results with the corresponding results available in literature shows successful implementation of the present method. The various graphical results are displayed at different time for different parameters such as nonlocal parameter, length scale parameter and non-negative ramp time parameter. The significant findings of the current work are listed below:

- By increasing small-scale parameter $e_0 a$, a stiffness-softening effect is produced. On the contrary, an increase in the length-scale parameter l_s produces stiffness-hardening.

- The peak of deflection rises and the frequency of oscillation deduces as the value of nonlocal parameter $e_0 a$ ascends.

- Stiffness hardening produces lower amplitude of deflection and increases vibration frequency with intensifying strain gradient length scale parameter l_s.

- The range of dimensionless deflection maximizes by increasing the aspect ratio of the beam's length-to-height ratio (L/h).

- The nonlocal beam theory (NBT) exhibits the highest deflection amplitude under MGT model, while the strain gradient theory depicts a less range of dimensionless deflection. It can be concluded that the declination of vibration frequency is maximum under nonlocal beam theory. However, the temperature changes under all the elasticity theories coincide with each other.

- With a rise in ramp time parameter t_0, the non-dimensional deflection and temperature changes in the beam resonator decrease.